APPLICATION OF MORPHOLOGICAL FILTERS IN ULTRASONIC FLAW DETECTION

M. A. MOHAMED and J. SANIIE

Department of Electrical and Computer Engineering
Illinois Institute of Technology
Chicago, IL 60616

ABSTRACT

Mathematical morphology has recently been introduced as a powerful tool for studying the geometrical properties of one or two dimensional signals. In this study, we have applied morphological filters to detect flaw in ultrasonic signals contaminated by grain scattering noise (i.e., speckles). In particular, the deterministic and stochastic properties of morphological filters have been studied in the context of utilizing different structuring elements. The structuring elements have been characterized by their shape, width, and height. We have used the information content of ultrasonic signals to design a suitable structuring element to enhance flaw-to-clutter ratio. The processed experimental results show that morphological filters can detect flaw echoes while suppressing microstructure noise.

INTRODUCTION

Morphological filters are a class of nonlinear filters that have recently become popular in signal processing for noise reduction, shape representation and recognition, skeletonization, and coding [1 - 5]. The word morphology refers to the study of forms and structures. Matheron [6] and Serra [7] introduced the theoretical foundation for mathematical morphology. In mathematical morphology [8 - 9], a signal is viewed as a set and is operated on by several set-processing morphological operations using structuring elements which are some-what simpler in nature than the signal under study. By varying the structuring element we can extract different types of information from the signal.

In order to examine the performance of morphological filters and capitalize on their applications, both deterministic and statistical analyses are needed. This paper evaluates the deterministic and stochastics properties of morphological filters when applied to ultrasonic signals (A-scan or B-scan) for flaw detection and signal-to-clutter ratio improvement.

THEORETICAL BACKGROUND

The primitives of morphological operations are erosion and dilation. Other morphological operations such as opening and closing are sequences of combining erosion and dilation. These operations can be applied to binary or multilevel signals. Since, ultrasonic backscattered echoes are multilevel signals, we therefore present a discussion of multilevel morphological operations.

Let x and s denote two discrete functions defined on X={0,1,.......,N-1} and S={0,1,.......,M-1}, respectively. It is further assumed that N>M. The multilevel dilation of signal x by a multilevel structuring element s is denoted by $x \oplus s$, and is defined as:

$$(x \oplus s)(m)=MAX_{n=m-M+1,........,m}\ \ x(n)+s(m-n), \tag{1}$$

where m= M-1, M, .., N-1.

Dilation is an "expansion" operation in that values of $x \oplus s$ are always greater than those of x. The multilevel erosion of a signal x by a multilevel structuring element s is denoted by $x \ominus s$, and is defined as:

$$(x \ominus s)(m)=MIN_{n=0,...,M-1}\ \ x(m+n)-s(n), \tag{2}$$

for m = 0, ..., N-M.

Erosion is a "shrinking" operation in that values of $x \ominus s$ are always less than those of x.

The multilevel opening of x, by structuring element s, is

$$x \ o\ s=(x \ominus s)\oplus s \tag{3}$$

The multilevel closing of x, by structuring element s, is

$$x \bullet s = (x \oplus s) \ominus s. \tag{4}$$

In general, an opening is used to suppress positive pulses while a closing is used to suppress negative pulses. Morphological operators are usually applied in sequence. Open-closing (OC) and clos-opening (CO) are two types of morphological filters used for noise suppression [5]. By using these filters we can obtain smoothed versions of the original signal , as they have some interesting properties in relation to median filters [10]. In particular, the open-closing and clos-opening give us median roots in a single pass [11], smooth signals similar to the median and are computationally more efficient.

DETERMINISTIC PROPERTIES OF MORPHOLOGICAL FILTERS

In order to properly apply morphological filters to ultrasonic signals, we examined their deterministic and stochastic properties using different structuring elements. The structuring element is characterized by its width (length), height, and shape.

To evaluate the performance of morphological filters for noise suppression and single echo detection, a sampled Gaussian envelope ultrasonic echo modeled as:

$$x(n)=e^{-\alpha n^2}\cos(2\pi f_c n) \tag{5}$$

was used. The term α is proportional to the bandwidth of the echo and f_c is the center frequency. In this simulation α=0.0002 and the number of samples per cycle of the ultrasonic echo is 80 (i.e., sampling rate is equivalent to $80 f_c$). The signal to be processed is a sum of two components: Gaussian envelope echo and uniformly distributed noise,

$$\hat{x}(n)=x(n)+\nu(n) \tag{6}$$

where ν(n) is a sequence of independent, identically distributed random variable signals with a uniform density function {-1/2, 1/2} resulting in a signal power to noise power ratio of 2.22 (SNR=3.477 dB).

An estimate of the signal is obtained by processing the input signal using an opening followed by a closing operation. A second estimate of the signal is formed by processing the input signal using a closing followed by an opening operation. Then the output signal y(n) is the average of these two estimates, i.e.,

$$y(n)=[(\hat{x}(n)\ o\ s)\bullet s+(\hat{x}(n)\bullet s)\ o\ s]/2. \tag{7}$$

The average of the two signals is used to minimize the bias caused by the extensiveness properties of opening and closing.

The algorithm presented in Equation (7) using sinusoidal structuring elements with a height= 0.1 and different widths (M= 3, 7, 11, 15, 19) is applied to the input signals (Equation (6)) and results are shown in Figure (1). Figure (1a) is original signal, Figure (1b) is signal plus noise, and Figure (1c - 1g) represents the processed results using different widths (M=3, 7, 11, 15, 19). This figure shows the effectiveness of the algorithm in suppressing noise and preserving the original echo. Also, the noise suppression increases while increasing the width of the structuring element, but the echo signal is attenuated when M>15. Figure (2) shows a comparison between the original echo signal with the processed output signal for width M=15. The signal-to-noise ratio after processing is 26.96, (i.e., SNR=14.30 dB). This means that the morphological filter improved the SNR by 10.83 dB.

If a signal with a certain frequency is unmodified by the application of morphological filters, any signals with a lower frequency will also be unmodified. It is also well known that sequentially alternating the application of opening and closing with the same structuring element removes details of the signal which are small relative to this structuring element. Using classical terminology, we can denote these alternating sequential filters (see Equation (7)) as morphological low-pass filters. This idea can be extended to design high-pass and band-pass filters. The high-pass filter can be designed using the original

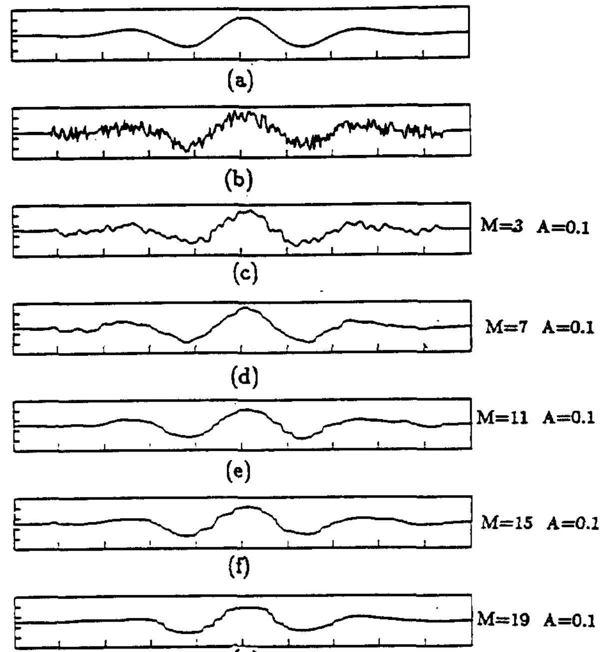

Figure (1) Echo detection and noise suppression using morphological operations.

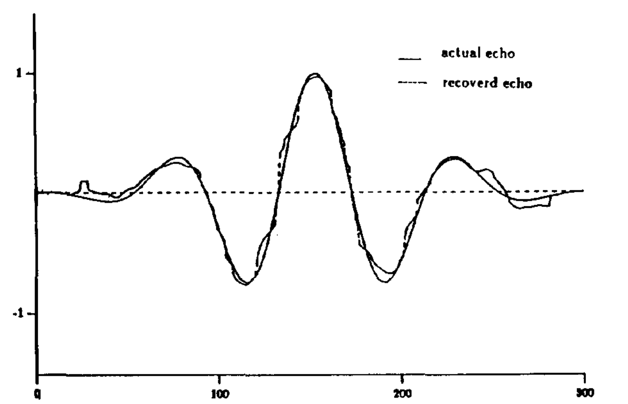

Figure (2) Comparison of the actual echo and the recovered echo using morphological filters.

signal minus the average of open-closing and clos-opening Finally, the band-pass filter is the difference of two averages of open-closing and clos-opening operations with two different structuring elements.

STATISTICAL PROPERTIES OF MORPHOLOGICAL FILTERS

Statistical expressions for dilation and erosion can be derived utilizing the relationship between morphological filters and order statistic(OS) filters [11]. This will provide insights into nonlinear behavior and the smoothing characteristics of morphological filters.

Equations (1) and (2), describing the dilation and erosion expressions, are related to OS filters. Suppose we sort M numbers in ascending order with respect to their algebraic value within a window size of length M. Then, the Mth OS of any signal coincides with dilation by a structuring element with a width M and a constant value zero, and the first order statistic (1st OS) coincides with erosion by a structuring element with a width M and a constant value zero.

The expression for the distribution function of dilation can be derived using the statistical property of the Mth OS. Let's assume that X_1, X_2, ..., X_M are M independent and identically distributed (iid) variates, each with a cumulative distribution function F(x). Then, the distribution function of dilation by a flat structuring element with a width M and a constant value zero becomes:

$$F_d(x) = F^M(x) \tag{8}$$

The density function of dilation p_d(x) can be found by taking the derivative of Equation (8) with respect to x,

$$p_d(x) = M\, F^{M-1}(x)\; p(x) \tag{9}$$

where p(x) is the density function of the input X_i.

If a flat structuring element has a width M and a constant value A, then the density function of dilation becomes:

$$p_d(x) = M\, F^{M-1}(x-A)\; p(x-A) \tag{10}$$

Calculation of the density function of dilation for independent and identically distributed inputs can be generalized to any structuring element by modifying the density function of the variates of the input signal. The modification is performed by shifting each density function to the right by a value depending on the values of the structuring element. The density function of dilation can be calculated using the statistical property of the Mth OS

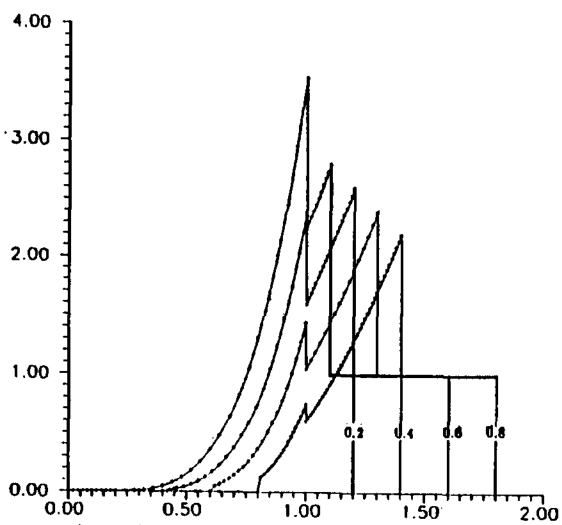

Figure (3) Dilation density function for a triangular structuring element.

density function for independent and non-identically distributed variates [12]. Therefore, the dilation density function by any structuring element becomes

$$p_d(x) = [\Pi_{i=1}^{M} F_i(x)] \sum_{i=1}^{M} \left(\frac{p_i(x)}{F_i(x)}\right) \tag{11}$$

where $p_i(x)$ and $F_i(x)$ are the modified density and distribution functions of the input signal according to the values of the structuring element. As an example, let's assume that the structuring element has a width, M= 5, and a triangular shape with height A. Using Equation (11), the dilation density function for uniform distribution inputs within the range of zero and one, for M=5, and $0 \le A \le 1$, can be obtained,

$$p_d(x) = \begin{cases} x(x-A/2)(5x^2-5.5Ax+A^2) & A \le x \le 1 \\ (x-A/2)(3x-2.5A) & 1 \le x \le 1+A/2 \\ 1 & 1+A/2 \le x \le 1+A \\ 0 & \textit{otherwise} \end{cases} \tag{12}$$

An evaluation of Equation (12) for uniformly distributed inputs and four different heights (A=0.2, 0.4, 0.6 and 0.8) of triangular structuring elements is shown in Figure (3), indicating that the density function of dilation depends on the density of the input signal, the shape, height and width of the structuring element. The effect of these parameters on the output dilation density function can be summerized as follows :

- The output density function is shifted to the right and the shift increases when the height A of the structuring element increases.
- The change in the overall shape of the input density function due to dilation is less affected by increasing the height of the structuring element.
- The variance of the output density function increases by increasing the height A, i.e., the output signal resembles more closely the original signal by increasing the height.
- The variance of the output density function decreases as window size (M) increases, and the increased window size facilitates a smoothed output.

The expression for the erosion density function can be derived using a similar method applied to the derivation of the dilation density function. This expression is derived using the statistical properties of the 1st OS. Suppose that a triangular shape has a width, M=5 and a height A. Then, the erosion density function of uniform, independent and identically distributed inputs can be obtained by replacing x with (1-x) in Equation (12). Note that the effect of the parameters of the structuring element on the erosion density function of uniform and identically distributed variates is the same as that of the dilation density function due to the symmetry of their expressions. The erosion density function is concentrated toward the lower values rather than the higher values in the dilation density function.

MORPHOLOGICAL FILTERS FOR FLAW DETECTION

Ultrasonic flaw detection is an important application of morphological filters. The goal in detection is to isolate the flaw echoes from background noise (e.g, speckles or microstructure scattering echoes) and to estimate flaw size and location. This section focuses upon the selection of morphological filters to detect flaw (i.e., target) in the ultrasonic imaging of complex structures with high scattering noise (clutter).

To illustrate the effectiveness of the parameters of the structuring element in detection, ultrasonic flaw signals contaminated by clutter have been studied. A broadband transducer was used to test a simulated flaw embedded within a steel block. Measurements were accomplished using the contact technique and data was acquired with a 100 MHz sampling frequency. An example of an experimental measurement of a broadband signal is shown in the top trace of Figure (4). The backscattered signal consists of multiple interfering echoes with random amplitudes and phases representing microstructural scattering. The ultrasonic flaw signal is masked by echoes scattered from the microstructure making detection very difficult. This signal was processed by the same sequence of opening and closing operations discussed in the previous section (Equation 7). Processed results are shown in Figure (4) for a flat structuring element with different widths (A=3, 4, 5, 6, 7, 8 samples). These results indicate that morphological filters are capable of detecting targets echoes while suppressing clutter.

In order to achieve a better evaluation of morphological filters, the effect of the parameters of structuring elements in detecting ultrasonic signals was examined using two different methods based on an evaluation of the zero crossing and flaw-to-clutter (F/C) ratio of the output signal.

In the first method, we calculated the number of zero crossings of the processed output signal with flat structuring elements for different widths. The result indicates that the number of zero crossings decreases when the width of a flat structuring element is increased. This simply implies that the smoothing process becomes more effective when the width of the structuring element is increased, although excessive smoothing may eliminate flaw echoes. Therefore, an evaluation of a zero crossing can lead to an estimation of the optimal width of the structuring element. The average width estimated with a zero crossing for the input signal is 5.14 which is very close to the optimal width, M_{op}=6, of the structuring element.

In the second method, the flaw-to-clutter ratio of the output signal as a function of the width of a flat structuring element is shown in Figure (5). This figure shows that the F/C increases as the width approaches the optimal value (M_{op}= 6). The F/C of the output signal at M_{op}=6 is 1.6 times (i.e., 2.05 dB) better than the F/C of the input signal.

To further improve the resolution and F/C ratio for flaw detection, it is effective to estimate the background noise

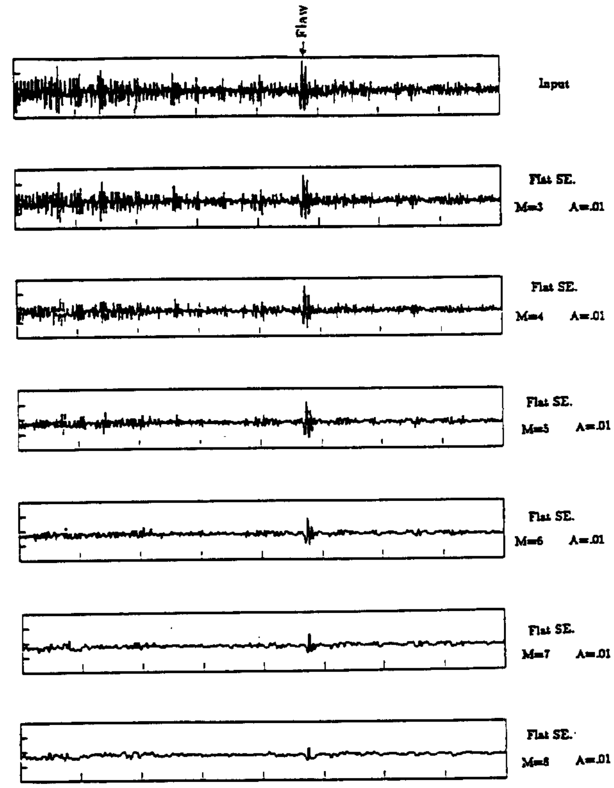

Figure (4) Processed outputs of a backscattered ultasonic signal. The top trace is the original measured signal.

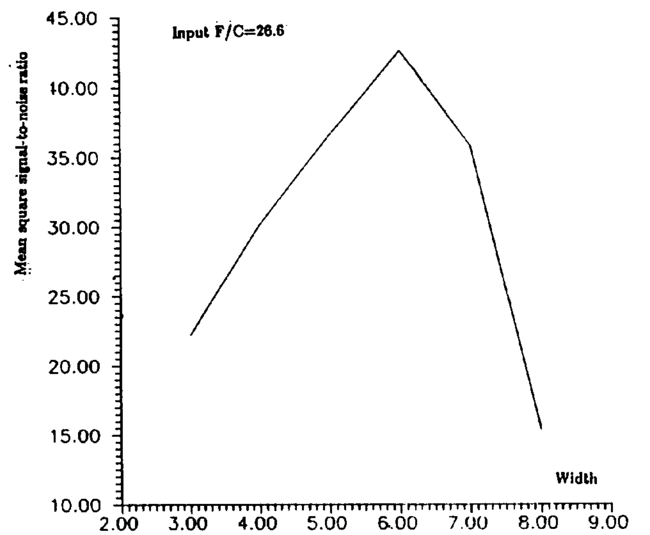

Figure (5) Flaw-to-clutter (F/C) ratio of the output signal as a function of the width of the structuring element.

and then subtract this estimate from the preprocessed signal. This technique is a band-pass filtering operation and can be represented as

$$\hat{y}(n)=y(n)-[(y(n)os_2)\bullet s_2)+(y(n)\bullet s_2)os_2)]/2 \qquad (13)$$

where

$$y(n)=[(\hat{x}(n)\ o\ s_1)\bullet s_1)+(\hat{x}(n)\bullet s_1)\ o\ s_1)]/2, \qquad (14)$$

The term $\hat{x}(n)$ is the measured utrasonic flaw echo corrupted by the microstructure noise, and s_1 and s_2 are flat structuring elements with lengths of 8 and 10 respectively. Processed results are shown in Figure (6). Comparison of Figure (6-a) (the measured signal) and Figure (6-b) (the processed signal) shows that the background noise is tremendously reduced, while the resolution is enhanced. The F/C is also improved by 5.66 dB.

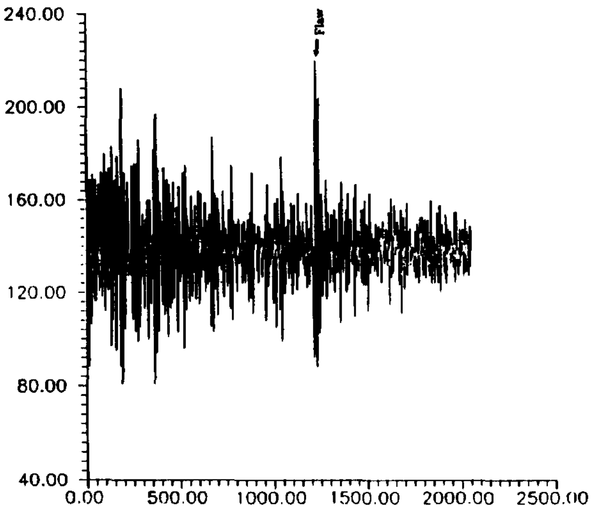

Figure (6-a) An ultrasonic backscattered flaw signal.

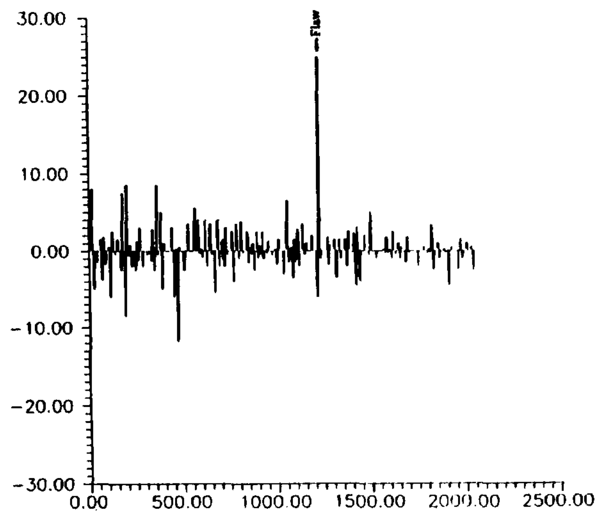

Figure (6) The processed output of a backscattered ultrasonic signal using the band-pass morphological filter.

CONCLUSION

This paper has dealt with the properties of morphological filters and their application for improving the flaw-to-clutter ratio of ultrasonic signals. Our study has focused on the deterministic and stochastic properties of morphological filters using different structuring elements. Structuring elements are characterized by their width, height and shape. From both a deterministic and a stochastic point of view, it has been shown that the filtering process depends on the input signal as well as the parameters of the structuring element. A mathematical expression for the dilation and erosion density function of independent and identically distributed inputs was derived using the statistical properties of order statistics filters. The processed experimental results show that morphological filters can detect flaw echoes while suppressing microstructure noise.

ACKNOWLEDGEMENTS

This project is supported in part by ONR contract Number S40000RB01, and the Electric Power Research Institute (EPRI) project number RP2614-75.

REFERENCES

[1] P. A. Maragos and R. W. Schafer, " Applications of Morphological Filtering to Image Analysis and Processing ", *Proc. ICASSP*, pp. 2067 - 2070, 1986.

[2] I. Pitas and A. N. Venetsanopoulos, " Morphological Shape Decomposition ", *Pattern Anal. Machine Intell.*, Vol. PAMI-12, no. 1, pp. 38 - 45, Jan. 1990.

[3] P. A. Maragos, and R. W. Schafer, " Morphological Skeleton Representation and Coding of Binary Image ", *IEEE Trans. Acoust.*, Speech, Signal Processing, Vol. ASSP - 34, pp. 1228 - 1244, oct. 1986.

[4] T. R. Crimmins and W. M. Brown, " Image Algebra and Automatic Shape Recognition ", *IEEE Trans. Aerospace and Electronic Systems,* Vol. AES-21, No. 1, 1985.

[5] C. H. Chu, E. J. Delp, " Impulsive Noise Suppression and Background Normalization of Electrocardiogram Signals Using Morphological Operators ", *IEEE Trans. Biomedical Eng.,* Vol.BME- 36, pp. 262 - 273, Feb. 1989.

[6] G. Matheron, *Random Sets and Integral Geometry,* New York: Wiley, 1975.

[7] J. Serra, *Image Analysis and Mathematical Morphology,* London: Academic, 1982

[8] R. M. Haralick, S. R. Sternberg, and X. Zhuang, " Image Analysis Using Mathematical Morphology", *IEEE Trans. Pattern Anal. Mach. Intell.*, Vol. PAMI-9, pp. 532 - 550, Jul. 1987.

[9] P. A. Maragos, and R.W. Schafer," Morphological Filters-Part I: Their Set-Theoretic Analysis and Relations to Linear Shift-Invariant Filters ", *IEEE Trans. Acoust., Speech, Signal Processing* , Vol. ASSP-35, pp. 1153 - 1169, Aug. 1987.

[10] N. C. Gallagher, JR., and G. L. Wise, " A Theoretical Analysis of Median Filters ", *IEEE Trans. Acoust., Speech, Signal Processing,* Vol. ASSP-29, pp. 1136 - 1141, Dec. 1981.

[11] P. A. Maragos, and R. W. Schafer, " Morphological Filters-Part II: Their Set-Theoretic Analysis and Relations to Linear Shift-Invariant Filters ", *IEEE Trans. Acoust., Speech, Signal Processing,* Vol.ASSP- 35, pp. 1170 - 1184, Aug. 1987.

[12] H. A. David, *Order Statistics,* New York: Wiley, 1981.